

Article

Six Sigma Analysis of Mini-Plate Fixation Systems Used in Human Mandible Fractures: A Clinical Case Study of Symphysis Fracture

Abdallah Shokry ¹, Ghais Kharmanda ², Hasan Mulki ^{3,*}, Mohamed Yaser Kharma ² and Saleh Mahmoud ³

¹ Department of Mechanical Engineering, Faculty of Engineering, Fayoum University, Fayoum 63514, Egypt; abdallah.shokry@fayoum.edu.eg

² 3D Printing 4U (UG), 51103 Cologne, Germany; ghais.kharmanda@3d-printing-4u.com (G.K.); mykharma@hotmail.com (M.Y.K.)

³ College of Engineering and Technology, American University of the Middle East, Egaila 54200, Kuwait; saleh.mahmoud@aum.edu.kw

* Correspondence: hasan.mulki@aum.edu.kw

Abstract: The objective of Six Sigma Analysis (SSA) is to determine the robustness level of a current design, process or system considering the expected range of an input parameter. This strategy has been successfully applied to several fields, including healthcare management. This work presents a novel study of SSA to assess the mini-plate fixation employed for mandible fracture. The objective is to reflect the number of concerns in a surgical operation case by performing a statistical measurement of operation capability. A three-dimensional finite element model of a clinical case is elaborated. Some muscles may be severed or damaged during surgery and unable to function to their full potential. To obtain reliable designs, these muscle forces are considered as random variables. The Six Sigma analysis is used to determine if the output parameters satisfy the Six Sigma quality criteria or not. The remarked potential failure modes in this study are found to be similar to those found in a previous reliability study that was applied to the same clinical case. According to the results of SSA, the assessment level ($2.462 \ll 6$) means that much of the data are outside of the demand, and require several improvements to ensure patient satisfaction.

Keywords: Six Sigma analysis; human mandible fractures; mini-plate fixation system



Citation: Shokry, A.; Kharmanda, G.; Mulki, H.; Kharma, M.Y.; Mahmoud, S. Six Sigma Analysis of Mini-Plate Fixation Systems Used in Human Mandible Fractures: A Clinical Case Study of Symphysis Fracture. *Appl. Sci.* **2023**, *13*, 12501. <https://doi.org/10.3390/app132212501>

Academic Editor: Gaetano Isola

Received: 19 September 2023

Revised: 7 November 2023

Accepted: 14 November 2023

Published: 20 November 2023



Copyright: © 2023 by the authors. Licensee MDPI, Basel, Switzerland. This article is an open access article distributed under the terms and conditions of the Creative Commons Attribution (CC BY) license (<https://creativecommons.org/licenses/by/4.0/>).

1. Introduction

For a given design case, using optimization algorithms for a single objective function alone does not render the best design, as it often results in a trade-off between several objectives [1]. In addition to the optimization algorithms, and in order to obtain better results, several techniques can be performed, such as probabilistic design [2], reliability assessment [3], and Six Sigma analysis [4]. In this work, the Six Sigma concept is used as an accurate tool to determine the robustness levels for a given case, which was first introduced by Carl Frederick Gauss (1777–1855) using the normal curve idea. In 1920, Walter Shewhart showed that three sigma from the mean provide the point at which a process requires correction [5]. However, the term “Six Sigma” belongs to a Motorola engineer named Bill Smith [6]. Six Sigma is an effective way to improve quality and performance [7,8].

According to a recent review of Niñerola et al. [9], this concept is used in healthcare to improve patient quality and safety; however, research was mostly carried out in the USA. Several works have been carried out to implement the Six Sigma approach in healthcare areas in order to improve the patient environments [10–17]. Additionally, a contemporary idea called Lean Six Sigma is utilized in healthcare to improve process capabilities and efficiency by diminishing wastes and faults [18]. In this work, it is applied to measure the defect rate in the mini-plate fixation strategy used in human mandible fractures, considering

a clinical case, with the objective of establishing an efficient strategy to improve the quality of surgical operations.

There are several possible reasons for mandible fracture, such as accidents caused by cars, motorbikes, and practicing sports. The mini-plates technique is one of the methods employed to fix fractured mandibles. In fact, due to surgery, some of the muscles might be cut or harmed, diminishing their performance. In order to produce dependable designs, there is a significant motivation to introduce loading uncertainties. Several works have integrated optimization and/or reliability concepts into this type of fixation. Kharmanda et al. [19] highlighted the importance of integrating muscle force during the early design and development phases. Next, Kharmanda and Kharma [20] incorporated structural optimization and reliability hypotheses into a fixation approach to a mini-plate, which is utilized in symphysis mandibular fractures, taking individual cortical tissue into account. Kharmanda et al. [21] examined a second clinical case of a mandible subjected to fracture to assess the reliability grade during convalescence, as well as healing phases, considering that bone is made up of cortical and cancellous tissues.

The primary objective of this work is to implement the Six Sigma to evaluate the quality levels of a surgical operation when using the mini-plate fixation method for a specific patient. This implementation represents a novel method. The Six Sigma analysis is used to determine whether the output parameters satisfy the Six Sigma quality criteria. In other words, an acceptable level of performance is necessary to ensure the patient's satisfaction. A numerical study is carried out of the present clinical case, and a statistical measurement is made based on the Six Sigma concept. The authors believe that using Six Sigma with fixation should be able to cover different reconstruction plates with different clinical cases, which will be taken into consideration in future publications.

2. Methods

2.1. Model Description

A 35-year-old male patient's orthopantomogram is shown in Figure 1a, which is implemented as a clinical example of a symphysis fracture. The fourth author performed the surgery at Aleppo University Hospital. In this surgery, two mini-plates of I type (Figure 1b) are utilized. The mini-plates that have five holes and four screws, which were implemented using the symphysis fracture, as shown in Figure 1a. Luckily, there were no specific treatment-related complications, and the recovery time was close to three months. In order to investigate the detrimental impact brought on by the stabilization of the fracture, a three-dimensional finite element model was employed. The model is built using a panorama of a 2D picture, with an estimation of the dimensions used to provide the section in SolidWorks. Finite element analysis was conducted using Ansys Workbench. Figure 1c shows the different boundary conditions and a section illustrates the bone tissues (cortical and cancellous bone tissues). Measuring the von Mises stresses, which are thought as a sign of mandibular fractures, at the end of the healing period, is intended to achieve acceptable rigidity.

2.2. Material Properties

As illustrated in Section A-A of Figure 1c, the mandible bone is composed of two tissues: cortical bone and cancellous bone tissues. The mechanical properties for the cortical tissue are $E = 15,750$ MPa and $\nu = 0.325$, and for cancellous tissue, the mechanical properties are $E = 300$ MPa, $\nu = 0.30$ [21]. In addition, the material properties of the used mini-plates and screws were assigned for titanium as follows: 110 GPa for Young modulus and 0.34 for Poisson ratio [22]. These were supplied from BIONIKA Medline Kft, Miskolc, Hungary. However, to compute the yield stress in tension, the optimized formulation proposed by Kharmanda [23] leads to $\sigma_T \in [90 \div 125]$ MPa for the cortical bone when considering the tension/compression ratio $R_{T/C} = [0.5 \div 0.7]$, and to $\sigma_T \in [3 \div 4]$ MPa for the cancellous bone when considering the tension/compression ratio $R_{T/C} \in [0.7 \div 1]$ [24].

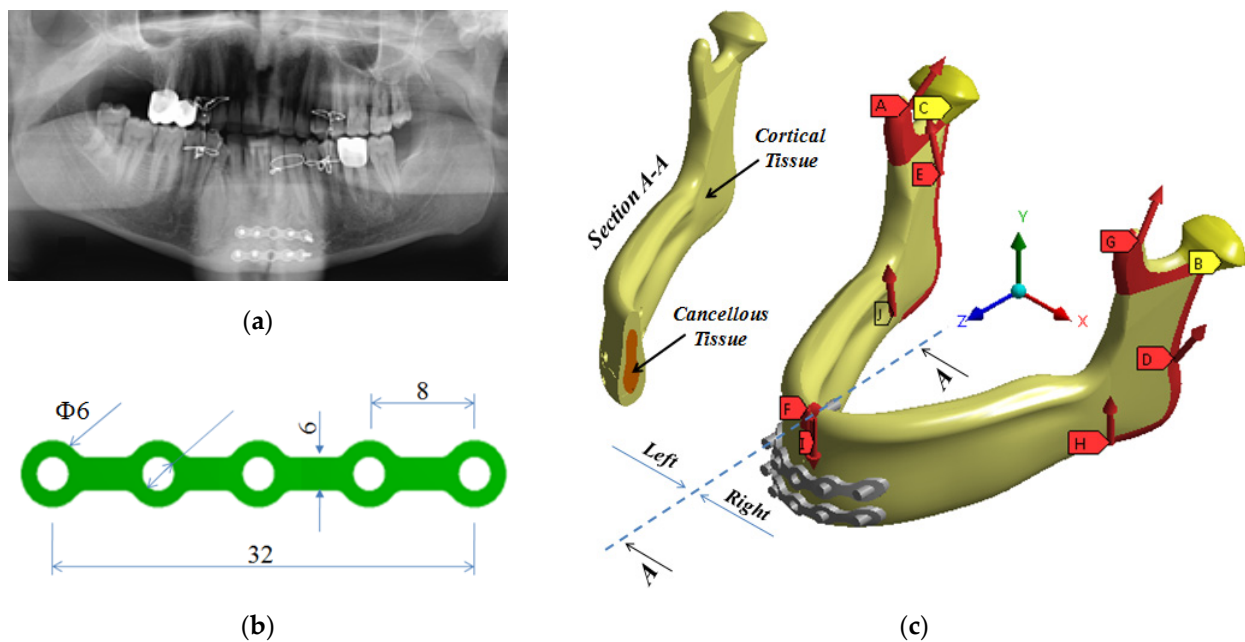


Figure 1. (a) A 35-year-old male patient's orthopantomogram, (b) dimensions of the mini plates in mm, and (c) finite element model with boundary conditions where the letters represent the locations of the applied forces as will be explained in Section 2.3.

2.3. Boundary Conditions

The model includes superficial masseter, deep masseter, anterior temporalis, medial temporalis, posterior temporalis, and medial pterygoid muscle forces. Table 1 shows the components of the utilized muscle forces, as introduced by Mesnard et al. [25].

Table 1. Muscle forces' components [25].

Muscle Forces	F_x (N)	F_y (N)	F_z (N)
superficial masseter	18.2	303.3	12.1
deep masseter	7.8	128.3	15.6
anterior temporalis	−18.4	104.8	−43.8
medial temporalis	−6.5	36.3	−53.1
posterior temporalis	−3.4	6.8	−37
medial pterygoid	187.4	325.1	−76.5

The digastric muscles are not very active during the bite operation, and are therefore ignored in the analysis [26]. Considering Figure 1c, the bite force is employed in areas *F* and *I*. The total masseter muscle forces of M^{Right} and M^{Left} are employed in areas *J* and *H*. The total temporal muscle forces are T^{Right} and T^{Left} , which are employed in areas *A* and *G*. Finally, the total pterygoid muscle forces are p^{Right} and p^{Left} , which are employed in areas *D* and *E*. The fixation of the mandible is located in areas *B* and *C*.

2.4. Six Sigma Strategy

The integration of Six Sigma into biomechanics can be considered a new aspect and more developments are needed before the Six Sigma methodology is adopted. As shown in Figure 2, five steps are used to solve problems: Define/Measure/Analyze/Improve/Control [8]. Each one of these five steps contains several actions depending on the field of application. The first step, 'Define', is related to the patient's needs. Here, the needs of the patient should be translated to quality characteristics. If we cannot define the quality characteristic of a

need, it is impossible to improve this need. In the second step, 'Measure', the objective is to identify the different opportunities for improvement when we determine intervals of variation. The third step, 'Analyze', is related to the process output (results), where the results should be understood to provide the patient's needs. In the fourth step 'Improve', we need to optimize the process where the objective is to identify the input variables that cause the most deviation from the target or the variation around the target. The final step, 'Control', seeks to verify the optimality settings where correlation and sensitivity analyses can help to identify the most effective parameters.

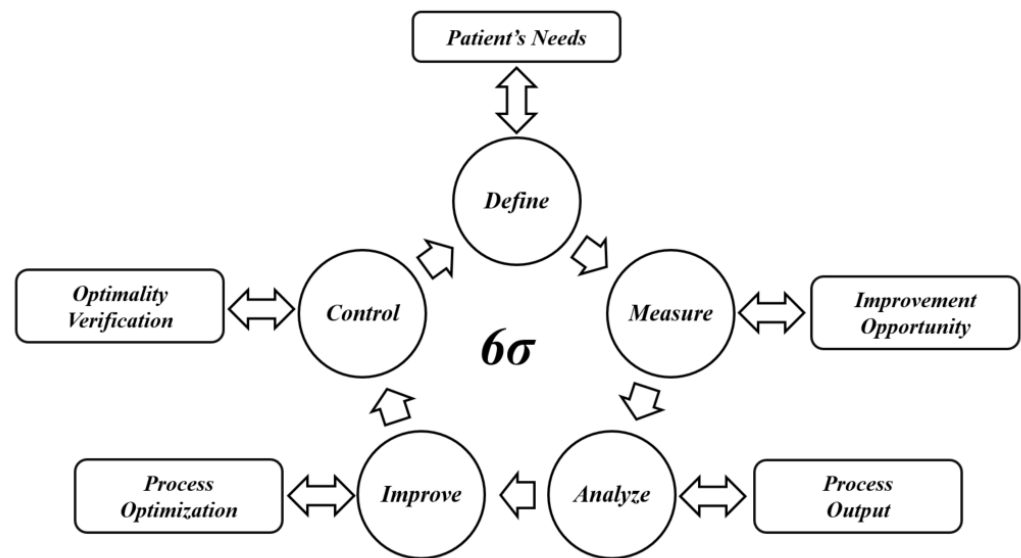


Figure 2. Six Sigma steps for surgical operations.

In simple terms, Six Sigma can be divided into two stages. The first stage is to improve quality by detecting defects in a design, process, or system, and to determine the causes of these defects, while the second stage is to increase the accuracy and repeatability by improving the studied design, process or system. Six Sigma analysis allows for the determination of whether the output parameters satisfy the Six Sigma quality criteria or not. In other words, the objective is to determine whether the current design meets the robustness requirements. For more details of the basic principles, the interested reader can refer to [27]. This section offers some details about Six Sigma analysis, where a normal distribution can be completely described using only the statistical parameters' mean and standard deviation. To identify whether the probability distribution follows the normal law or not, the middle distance between the maximum and minimum value of the quantile (Q_i^{max}, Q_i^{min}) can be measured. In this way, the middle distance can be written as:

$$Q_i^{middle} = \frac{Q_i^{max} + Q_i^{min}}{2} \tag{1}$$

if the mean value m_i is located at the middle distance ($m_i \approx Q_i^{middle}$), the probabilistic distribution follows the normal law.

In addition to describe the resulting distribution, two statistical measurements should be considered: the skewness ζ_i^S and the kurtosis ζ_i^K [28]. The skewness measures the distribution symmetry by determining the location of the majority of values. When the skewness value equals zero, the corresponding distribution is then symmetric. If the skewness value is positive, this means that the majority of the output values are closer to their minimum values and vice versa. When the skewness value is positive, the mean and median are greater than the mode and vice versa. Some approximations can be considered to identify the symmetry:

- $\zeta_i^S \in [-0.5 \div 0.5]$: the distribution is fairly symmetric.
- $\zeta_i^S \in [-1 \div -0.5[$ (negatively skewed) or $\zeta_i^S \in]0.5 \div 1]$ (positively skewed): the distribution is moderately skewed.
- $\zeta_i^S < -1$ (negatively skewed) or $\zeta_i^S > 1$ (positively skewed): the distribution is highly skewed.

The kurtosis measures whether the distribution is flat or steep relative to the normal distribution. The interpretation can be established as follows:

- $\zeta_i^K < 3$: the distribution is a flat curve.
- $\zeta_i^K = 3$: the distribution is a normal curve.
- $\zeta_i^K > 3$: the distribution is a steep curve.

In order to improve the current design, two processes are needed: sensitivity and correlation evaluations. Sensitivity evaluation helps to identify the most critical input parameters for certain output parameters (responses), while the correlation evaluation affects levels between the different parameters.

In addition, the problem’s nature should be modeled to allow for us to analyze the different results. In Figure 3, two problems are described: the first one concerns off-target problems and the second one concerns a variation problem.

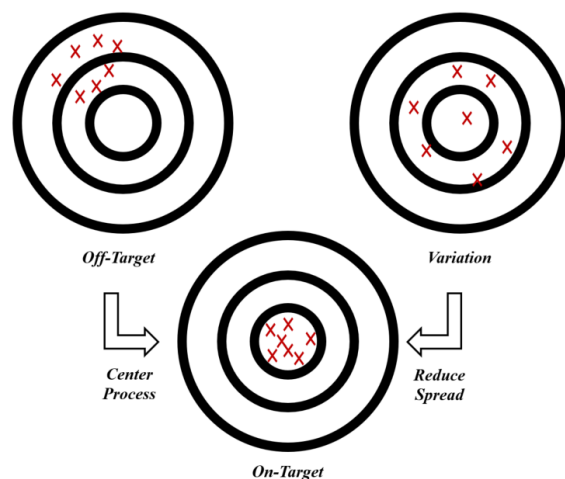


Figure 3. Improvement in process output, where × symbols represent the location of the data.

In this work, there are twenty input parameters that are regarded as random variables, two bite forces and eighteen muscle forces. Maximum von Mises stress points in the mini-plates (upper and lower), the cortical tissue (right and left parts) and the cancellous tissues (right and left parts) are the output parameters. The sampling type is LHS (Latin Hypercube Sampling) and the number of samples is 100. The sensitivity is captured through performance variability estimations.

3. Results

Considering the muscle force values that are provided in Table 1 and the value of bite force at the maximum capability of a normal mandible (un-fractured), the components of the forces as regards the chosen coordinate system are provided in Table 2, which represent the current design. Considering that the fracture indicator can be regarded as the maximum von Mises stress [29], the maximum value of von Mises stress is located at the cortical bone tissues, specifically at the right part with a value of $\sigma_{max}^{CorRight} \approx 71$ MPa (cf. Figure 4a). Consequently, the maximum displacement is found at the right part of the cortical bone tissue (cf. Figure 4b), with a value of $\delta_{max}^{CorLeftBack} \approx 0.3$ mm.

Table 2. Values of forces as well as related probabilistic parameters. MP: Mean Point and SD: Standard Deviation.

Input Parameters		Number	MP	SD	Min	Max
F^{Right} (N)	F_y^{Right}	P_1	−104	5.2	−200	−50
F^{Left} (N)	F_y^{Left}	P_2	−104	5.2	−200	−50
M^{Right} (N)	M_x^{Right}	P_3	26	1.3	2.6	26
	M_y^{Right}	P_4	431.6	21.58	43.16	431.6
	M_z^{Right}	P_5	27.7	1.39	2.77	27.7
M^{Left} (N)	M_x^{Left}	P_6	−26	1.3	−26	−2.6
	M_y^{Left}	P_7	431.6	21.58	43.16	431.6
	M_z^{Left}	P_8	27.7	1.39	2.77	27.7
T^{Right} (N)	T_x^{Right}	P_9	−28.3	1.42	−28.3	−2.83
	T_y^{Right}	P_{10}	147.9	7.40	14.79	147.9
	T_z^{Right}	P_{11}	−133.9	6.70	−133.9	−13.39
T^{Left} (N)	T_x^{Left}	P_{12}	28.3	1.42	2.83	28.3
	T_y^{Left}	P_{13}	147.9	7.40	14.79	147.9
	T_z^{Left}	P_{14}	−133.9	6.70	−133.9	−13.39
p^{Right} (N)	p_x^{Right}	P_{15}	187.4	9.37	18.74	187.4
	p_y^{Right}	P_{16}	325.1	16.26	32.51	325.1
	p_z^{Right}	P_{17}	−76.5	3.83	−76.5	−7.65
p^{Left} (N)	p_x^{Left}	P_{18}	−187.4	9.37	−187.4	−18.74
	p_y^{Left}	P_{19}	325.1	16.26	32.51	325.1
	p_z^{Left}	P_{20}	−76.5	3.83	−76.5	−7.65

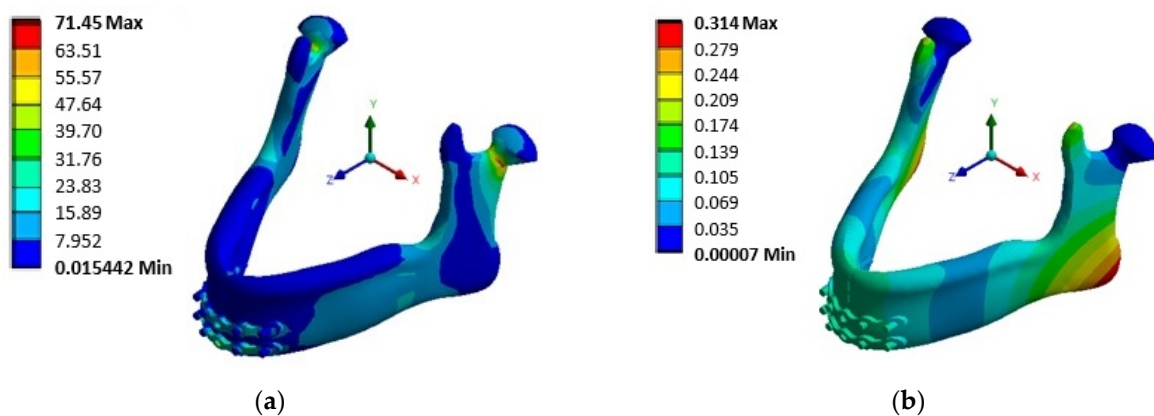


Figure 4. Distribution of (a) von Mises stresses in MPa, and (b) total displacements in mm.

The initial step of SSA is the Design Of Experiments (DOE), to build a Response Surface (RS) over the design space. The next step is to describe the variation range of the selected input parameters. The mean values are the forces applied to the current design with standard deviations of 5% (Table 2). All input parameters are normally distributed. Minimum and maximum values of forces are presented in Table 2.

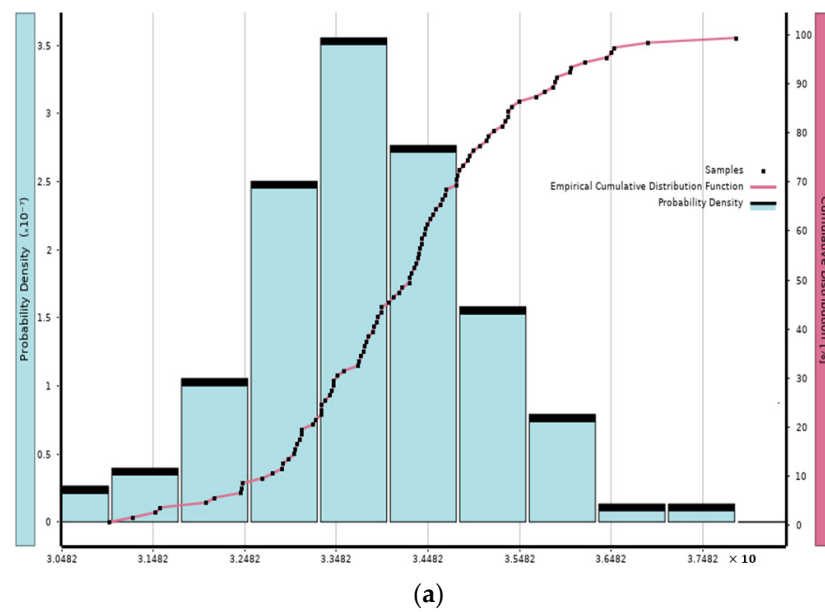
The minimum and maximum points regarding each parameter from the output parameters were roughly established through Min–Max search on the RS (cf. Table 3). According to the data presented in the table, the maximum values of von Mises stresses exceed the $\sigma_T = 90$ MPa for the cortical bone tissues, which was calculated using an optimized formulation that was proposed by Kharmanda [23].

Table 3. Output parameters and their probabilistic measurements.

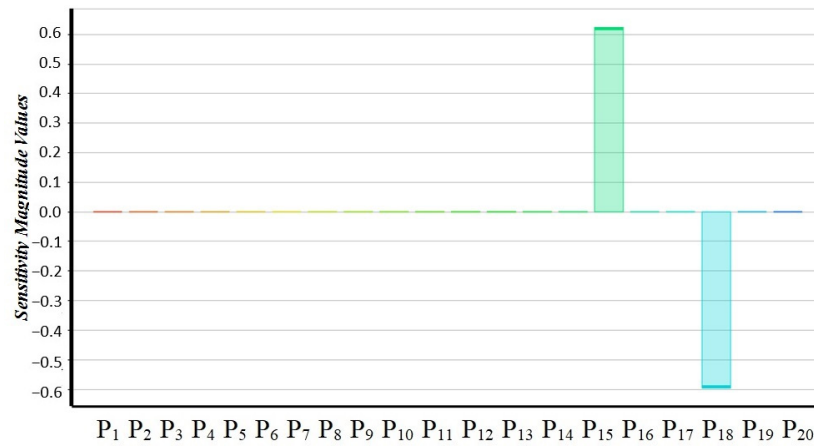
Parameters	$\sigma_{max}^{UppPlate}$	$\sigma_{max}^{LowPlate}$	$\sigma_{max}^{CanRight}$	$\sigma_{max}^{CorRight}$	$\sigma_{max}^{CanLeft}$	$\sigma_{max}^{CorLeft}$
CD	34.19	61.96	1.06	71.45	1.02	69.06
m_i	34.19	61.96	1.06	72.02	1.03	69.10
σ_i	1.25	2.06	0.34	3.14	0.62	3.11
ζ_i^S	0.03	0.07	0.06	0.96	−0.23	0.40
ζ_i^K	0.36	0.26	0.20	2.15	0.85	−0.05
Q_i^{min}	31.01	57.10	0.97	65.72	0.83	63.08
Q_i^{max}	37.85	67.84	1.15	83.90	1.19	77.18
Q_i^{middle}	34.43	62.47	1.06	74.81	1.01	70.13
V_i^{min}	24.13	45.09	0.77	19.44	0.54	44.13
V_i^{max}	44.21	78.85	1.34	152.90	1.56	94.83

Figure 5a represents the probabilistic distribution of the resulting maximum von Mises values of the upper mini-plate ($\sigma_{max}^{UppPlate}$). It can be observed that the probabilistic distribution does not follow the normal law. This observation is supported by the numerical results presented in Table 3, where the middle quantile values do not always equal to the mean value ($m_i \neq Q_i^{middle}$). Most of the maximum von Mises stress points are nearer to their minimum points, since the skewness point is positive ($\zeta_i^S > 0$). However, the distribution can be considered fairly symmetric, since the skewness equals $\zeta_i^S = 0.03 \in [-0.5 \div 0.5]$, while its curvature is considered highly flat since the kurtosis value is small: $\zeta_i^K = 0.36 < 3$. Figure 5b represents the sensitivity magnitude values of the resulting maximum von Mises values of the upper mini-plate with respect to the different force components. The most effective parameters are the medial pterygoid muscle forces in x direction (P_x^{Right} and P_x^{Left}). The right force component P_x^{Right} has a positive influence, while the left one has a negative effect. They have almost the same sensitivity values in opposite signs, and appear to meet the equilibrium condition.

Figure 6a represents the probabilistic distribution of the resulting maximum von Mises values of the lower mini-plate. It can also be observed that the probabilistic distribution does not follow the normal law. This observation is supported by the numerical results presented in Table 3, where the middle quantile values do not equal the mean value ($m_i \neq Q_i^{middle}$). Most of the maximum von Mises stress points are nearer to the minimum points, since the skewness value point is positive ($\zeta_i^S > 0$). However, the distribution can be considered fairly symmetric, since the skewness equals $\zeta_i^S = 0.07 \in [-0.5 \div 0.5]$, while its curvature is considered highly flat, since the kurtosis value is small $\zeta_i^K = 0.26 < 3$. Figure 6b represents the sensitivity magnitude values of the resulting maximum von Mises values of the lower mini-plate with respect to the different force components. In addition to the most important influence of the medial pterygoid muscle forces in x direction (P_x^{Right} and P_x^{Left}), both bite force components have a significant effect, although their effect is less than the previous muscle forces. The right force component P_x^{Right} has a positive influence, while the left one has a negative effect. On the other hand, both bite force components have a negative influence.



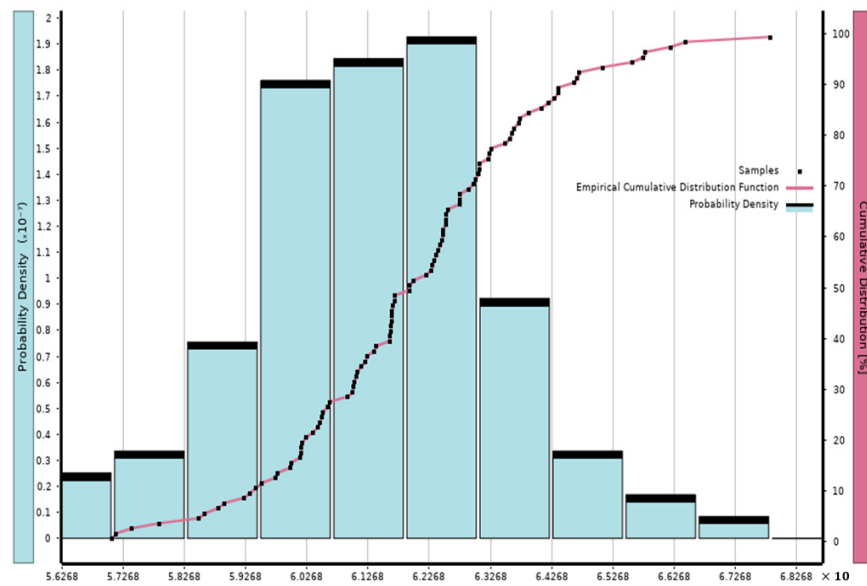
(a)



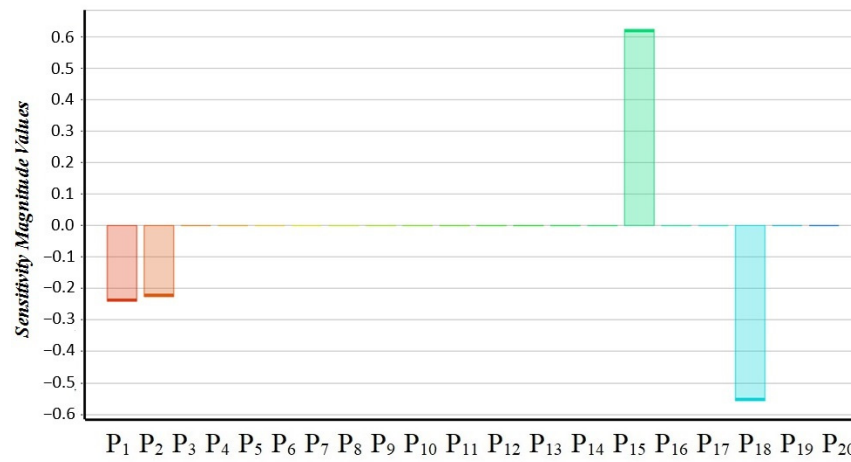
(b)

Figure 5. (a) Distribution of the resulting maximum von Mises values, (b) sensitivity magnitude values with respect to the different force components of the upper mini-plate.

Figure 7a represents a probabilistic distribution of the resulting maximum von Mises values of the right cancellous bone part. It can also be observed that the probabilistic distribution can be considered a normal curve. This observation is supported by the numerical results presented in Table 3, where the middle quantile values are equal to the mean value ($m_i = Q_i^{middle}$). The majority of the maximum von Mises stress values are closer to their minimum values, since the skewness value is positive ($\zeta_i^S > 0$). However, the distribution can be considered fairly symmetric since the skewness equals $\zeta_i^S = 0.06 \in [-0.5 \div 0.5]$, while its curvature is considered highly flat since the kurtosis value is small: $\zeta_i^K = 0.20 < 3$. Figure 7b represents the sensitivity magnitude values of the resulting maximum von Mises values of the lower mini-plate with respect to the different force components. In addition to the most important influence of the medial pterygoid muscle forces in x direction (P_x^{Right} and P_x^{Left}), both bite force components have a significant effect but less effect than the previous muscle forces. The right force component P_x^{Right} has a positive influence, while the left one has a negative effect. On the other hand, both bite force components have a negative influence.



(a)



(b)

Figure 6. (a) Distribution of the resulting maximum von Mises values, (b) sensitivity magnitude values with respect to the different force components of the lower mini-plate.

Figure 8a represents the probabilistic distribution of the resulting maximum von Mises values of the right cortical bone part. It can be observed that the probabilistic distribution does not follow the normal law. This observation is supported by the numerical results presented in Table 3 where the middle quantile values do not equal the mean value ($m_i \neq Q_i^{middle}$). Most of the maximum von Mises stress points are nearer to their minimum points, since the skewness point is positive ($\zeta_i^S > 0$). However, the distribution can be considered moderately skewed since the skewness equals $\zeta_i^S = 0.96 \in]0.5 \div 1]$, while its curvature is considered lightly flat since the kurtosis value is small: $\zeta_i^K = 2.15 < 3$. Figure 8b represents its sensitivity magnitude values of the resulting maximum von Mises values of the right cortical bone part with respect to the different force components. The most effective parameters are the right medial pterygoid muscle force component in the x direction (P_x^{Right}) and the right masseter muscle force component in direction y (M_y^{Right}). Both of them have a positive influence, while the right medial pterygoid muscle force component in x direction (P_x^{Right}) has a larger magnitude value than the other one.

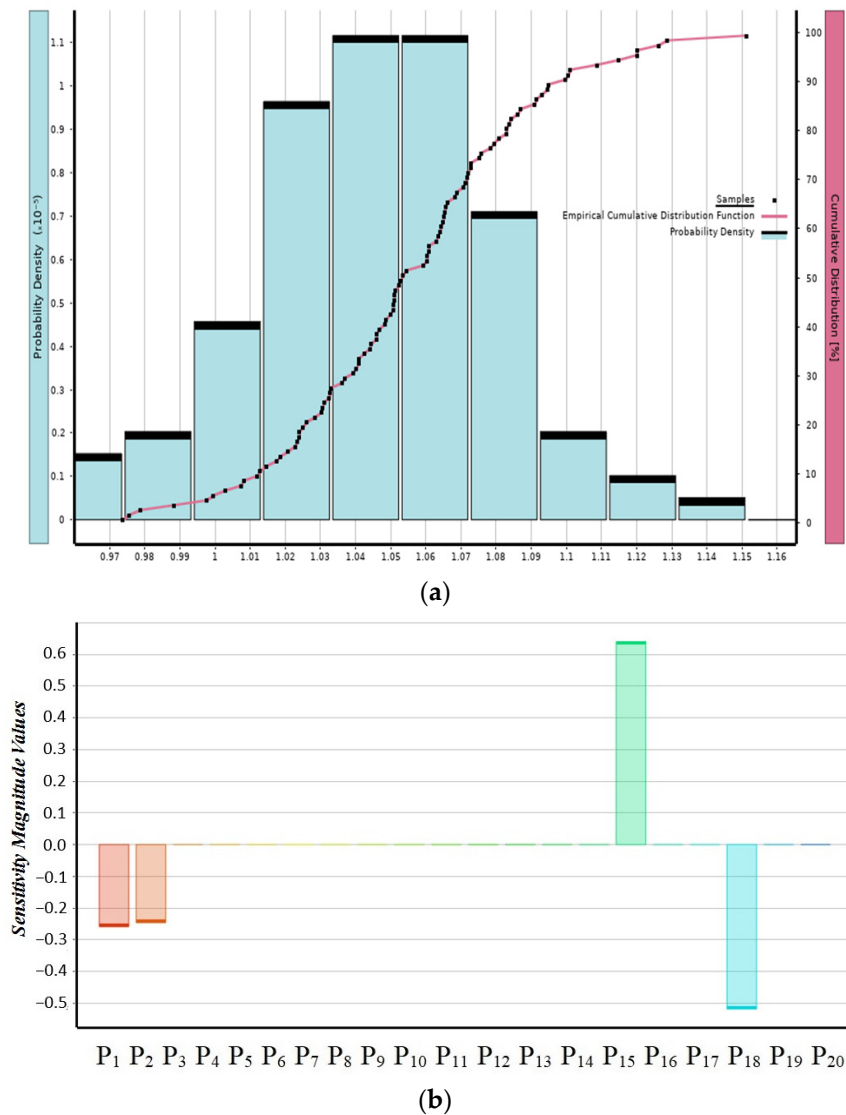
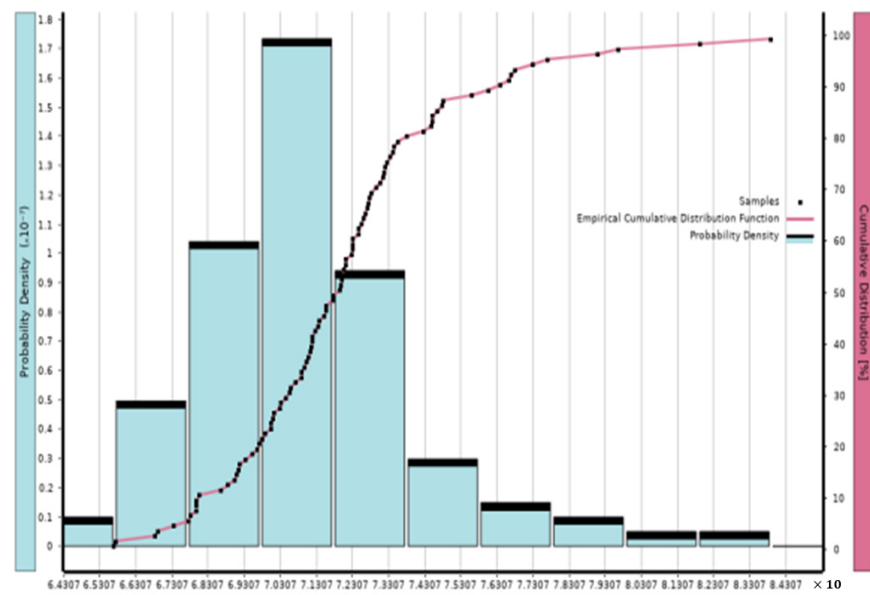
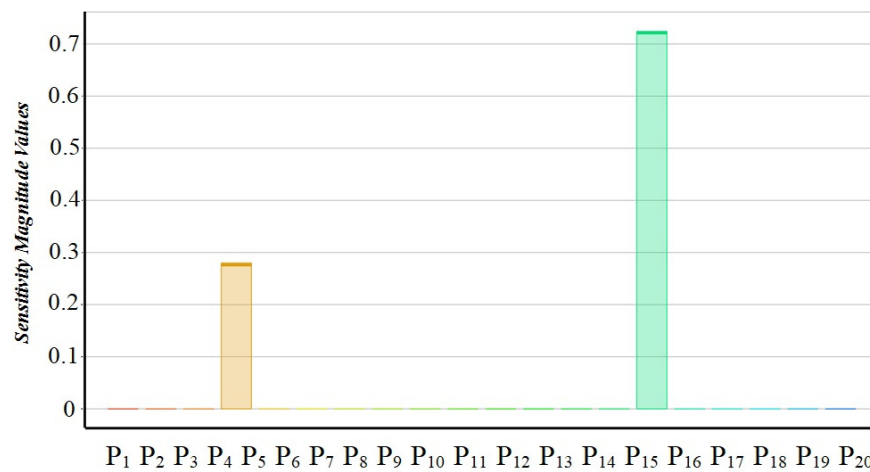


Figure 7. (a) Distribution of the resulting maximum von Mises values, (b) sensitivity magnitude values with respect to the different force components of the right cancellous bone part.

Figure 9a represents the probabilistic distribution of the resulting maximum von Mises values of the left cancellous bone part. It can be observed that the probabilistic distribution does not follow the normal law. This observation is supported by the numerical results presented in Table 3, where the middle quantile values do not equal the mean value ($m_i \neq Q_i^{middle}$). Most of the maximum von Mises stress points are nearer to their maximum points since the skewness point is negative ($\zeta_i^S < 0$). However, the distribution can be considered fairly symmetric since the skewness equals $\zeta_i^S = -0.23 \in [-0.5 \div 0.5]$, while its curvature is considered flat since the kurtosis value is small: $\zeta_i^K = 0.85 < 3$. Figure 9b represents the sensitivity magnitude values of the resulting maximum von Mises values of the left cancellous bone part with respect to the different force components. The most effective parameters are the left medial pterygoid muscle force component in x direction (P_x^{Left}), the right masseter muscle force component in direction y (M_y^{Right}), and the bite forces (F_y^{Right} and F_y^{Left}). Both of them have a negative influence, while the left medial pterygoid muscle force component in x direction (P_x^{Left}) has a larger magnitude value than the other forces.



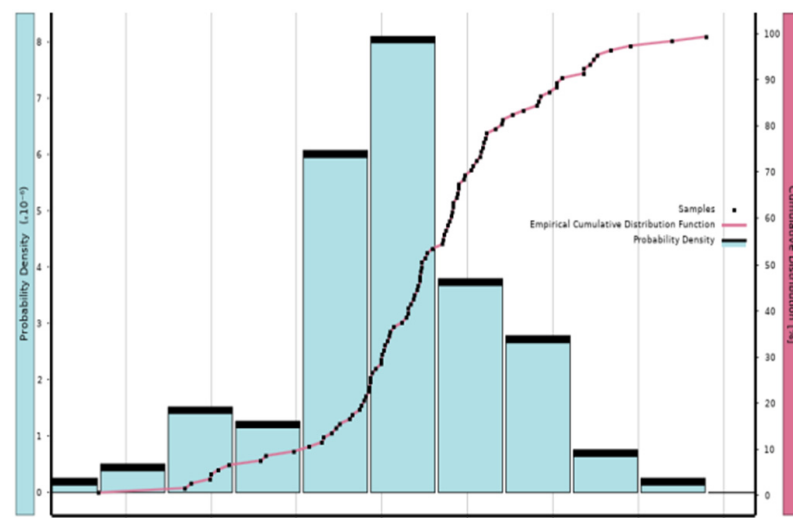
(a)



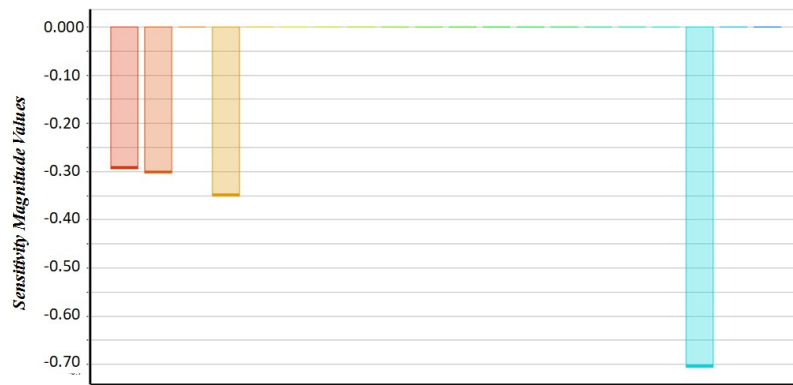
(b)

Figure 8. (a) Distribution of the resulting maximum von Mises values, (b) sensitivity magnitude values with respect to the different force components of the right cortical bone part.

Figure 10a represents the probabilistic distribution of the resulting maximum von Mises values of the left cortical bone part. It can be observed that the probabilistic distribution does not follow the normal law. This observation is supported by the numerical results presented in Table 3, where the middle quantile values do not equal the mean value ($m_i \neq Q_i^{middle}$). Most of the maximum von Mises stress points are nearer to their maximum points since the skewness point is negative ($\zeta_i^S < 0$). However, the distribution can be considered fairly symmetric since the skewness equals $\zeta_i^S = 0.4 \in [-0.5 \div 0.5]$, while its curvature is considered highly flat since the kurtosis value is small: $\zeta_i^K = -0.05 < 3$. Figure 10b represents the sensitivity magnitude values of the resulting maximum von Mises values of the left cancellous bone part with respect to the different force components. The most effective parameters are the left medial pterygoid muscle force component in x direction (P_x^{Left}) and the left masseter muscle force component in direction y (M_y^{Left}). The left medial pterygoid muscle force component in x direction (P_x^{Left}) has a negative influence, while the other force component has a positive effect. It has also a larger magnitude value than the other force.

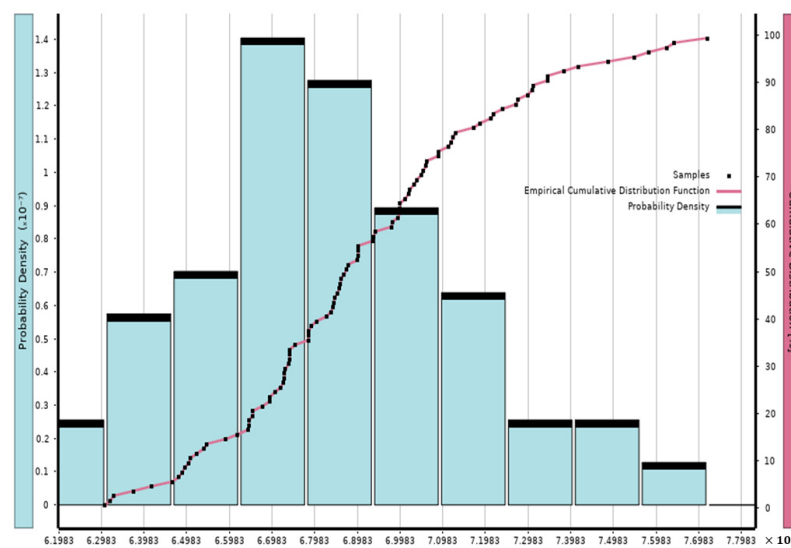


(a)



(b)

Figure 9. (a) Distribution of the resulting maximum von Mises values, (b) sensitivity magnitude values with respect to the different force components of the left cancellous bone part.



(a)

Figure 10. Cont.

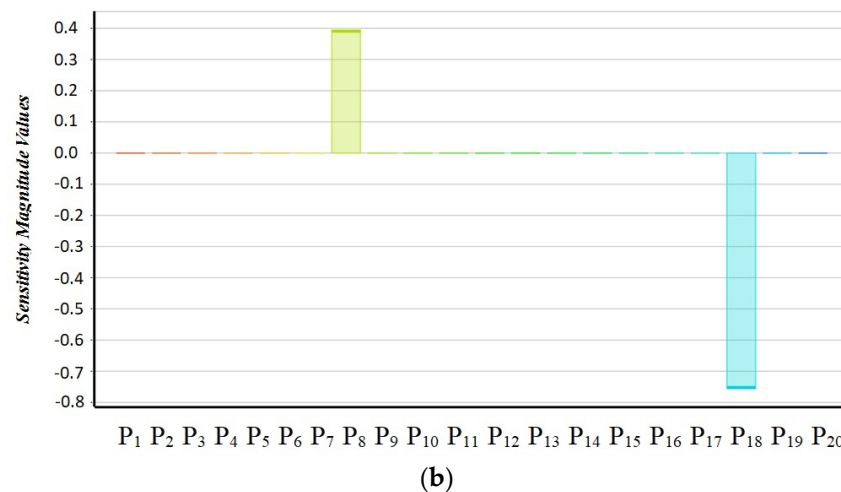


Figure 10. (a) Distribution of the resulting maximum von Mises values, (b) sensitivity magnitude values with respect to the different force components of the left cortical bone part.

4. Discussion

Several points need to be discussed to improve the quality levels in order to fulfill the patient's needs. First, sensitivity analyses are an important tool to determine the effect of input parameters of the responses. It is shown that the left medial pterygoid force in the x direction has a big influence on all output parameters except the maximum von Mises stress points of the cortical tissue in the right mandible part. Figure 11a provides the maximum von Mises stress values on the different mandible parts, while Figure 11b shows the sensitivity values regarding the effective forces at each mandible parts. Here, it can be found that the bite forces only have a large influence (negative effects) on the maximum von Mises stress points of the cancellous in the right and left mandible parts, and on the lower mini-plate. The right medial pterygoid force (P_{15}) in the x direction has a significant influence on all the different output parameters except the maximum von Mises stress points of the cortical and cancellous tissues in the left mandible parts. The right superficial masseter force (P_4) in the y direction only influence the maximum von Mises stress points of the cortical tissue in the right mandible part. The left superficial masseter force (P_7) in the y direction only has an influence on the maximum von Mises stress points of the cortical tissue in the left mandible part.

Furthermore, the results show that the output parameters do not satisfy the Six Sigma quality criteria. The assessed value σ -level ± 2.462 , which corresponds to a minimum probability of 0.7% and to a maximum probability of 99.3%. The skewness values of all output parameters (except the maximum von Mises stress values of the cancellous tissue in the left mandible part) are positive, which means that most of the maximum von Mises stress points are nearer to their minimum values. SSA helps to determine the critical point of the studied case to find additional improvements [30]. In several distribution diagrams, much of the data are outside of the patient's need. The whole point of Six Sigma is to work with the variation and the center to make improvements.

Improvements can be discussed either clinically or numerically. In order to improve the design quality, the choice of fixation method (two mini-plates and four screws for each) is first clinically justified. The mandibular bone is exposed to many kinds of linear and angular forces underload, such as compression and tension, shear, torsion, and bending. External forces cause mandibular bone to undergo plastic and elastic deformations. On the other hand, muscles exert some vertical and horizontal forces on fragments. These forces may cause the displacement of fragments or may act as a stabilizer for fragments. The temporalis, masseter, and medial pterygoid muscles pull are responsible for the vertical displacements of fragments. Horizontal displacements are mainly caused by lateral and

medial pterygoid muscle pull. Some muscles exert a complex force on fragments such as mylohyoid, digastric, and geniohyoid, which have a torsion effect on fragments [31,32].

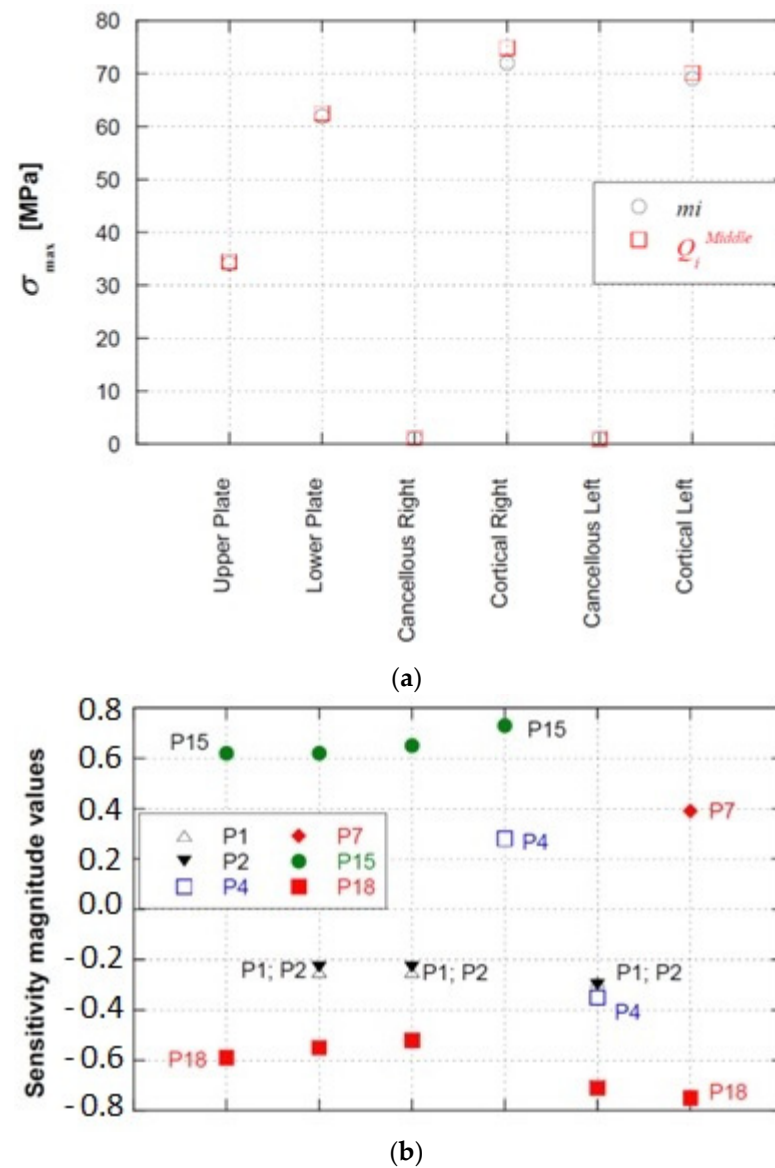


Figure 11. (a) Maximum von Mises stress, and (b) sensitivity values for mandible parts.

Champy and co-workers described a zone of tension in the alveolar part of the mandible and a zone of compression on the lower border [33], as shown in Figure 12. This information allows for ideal lines for mandibular internal fixation to be identified along the physiological tension lines. The tension and compression zones' pulling force, as applied by muscles of the oro-maxillofacial region, creates a zone of compression and tension within the mandible. The superior portion of the mandibles is termed the tension zone, and the inferior portion is termed the compression zone. Champy's principle of osteosynthesis lines is based on this tension. Therefore, according to Champy, the principle of osteosynthesis is to re-establish the mechanical qualities of the mandible. Hence, two miniplates were used in the anterior region: one at the inferior border, and the other 5 mm above the lower plate.



Figure 12. Principle of Champy for osteosynthesis lines.

According to this clinical analysis, there are no significant improvements to be made, while the simplification of the numerical model and the use of finite element simulation play an important role in the results. In a recent study by Graillon et al. [34], the researchers carried out a direct finite element study and recommended informing the patient of the potential risks, while we propose checking the accuracy of the finite element study that is used. For the current model, we have to reduce the variation in the following outputs: $\sigma_{max}^{UpperPlate}$ (the resulting maximum von Mises values of the upper mini-plate), $\sigma_{max}^{LowerPlate}$ (the resulting maximum von Mises values of the lower mini-plate), and $\sigma_{max}^{CanRight}$ (the resulting maximum von Mises values of the right cancellous bone part) in order to improve the quality of SSA.

In addition, it is possible to use topology optimization techniques to find the best distribution of the mini-plates and screws, considering the principle of Champy as optimization constraints. The interested reader can find some ideas in [35] regarding the integration of topology optimization techniques into mini-plate fixation.

In this work, most of the damage in the mandible affects its front part. In the work of Atilgan et al. [36], for young patients, the most common fracture site was the condyle (36%), followed by symphysis/parasymphysis (35%). Considering adults, the most frequent site was the symphysis/parasymphysis (36%), followed by the condyle (20%) and body (20%). However, in a recent study by Frimpong et al. [37], the most frequent site in adults was parasymphysis (37.2%), followed by the body (26.8%) and the condyle (17.2%).

The application of traditional reconstruction plates to a specific patient to evaluate the quality of a performed surgical operation, and the lack of different clinical cases, can be considered a limitation. The strategy should be applied to a wider group of patients in order to increase its reliability. Another limitation is the simplification of the geometrical description of the CAD model, considering a 2D panorama picture. For future works, additive manufacturing can be added to fabricate the fractured mandible in order to simulate the surgical operation, and Design For Six Sigma (DFSS) can be used to improve the quality.

5. Conclusions

The novelty of this work is the implementation of Six Sigma analysis when considering the mini-plate fixation approach in human mandible fractures. The results led to an evaluation of sigma level in the studied clinical case, where the assessed value does not meet the Six Sigma requirements. Several points are considered to understand the different causes of these low-quality levels, which provides the reader with an analytical analysis that can be used to improve the quality levels of a specific surgical operation. Another concept, called

Design for Six Sigma (DFSS) “Robust Design”, is then required in the upcoming study to enhance design quality by reducing performance variations.

The work presented in this study can be considered a foundation for future research in this area. To reduce or prevent potential failure modes, several factors can be taken into account: type of fracture, location of fracture, technique of treatment, teeth support, etc. In future work, the Failure Mode and Effect Analysis (FMEA) can be integrated as a systematic method to detect the different failure modes and to reduce the consequences of those failures as much as possible. Despite the Six Sigma strategy requiring more computing time to be performed, it leads to more accurate results relative to the other approximation methods.

Author Contributions: Conceptualization, G.K., A.S. and M.Y.K.; Methodology, G.K. and H.M.; Software, A.S. and G.K.; Validation, A.S., G.K. and H.M.; Formal Analysis, A.S. and G.K.; Investigation, A.S. and G.K.; Resources, M.Y.K. and S.M.; Data Curation, H.M. and S.M.; Writing—Original Draft Preparation, A.S., G.K. and H.M.; Writing—Review and Editing, A.S., G.K. and M.Y.K.; Visualization, G.K., A.S. and M.Y.K.; Supervision, G.K. All authors have read and agreed to the published version of the manuscript.

Funding: This research received no external funding. The APC was funded by College of Engineering and Technology of the American University of the Middle East, Kuwait.

Institutional Review Board Statement: Not applicable.

Informed Consent Statement: This article does not contain any studies with human participants performed by any of the authors but only using a model that is built using a panorama of a 2D picture, with an estimation of the dimensions used to provide the section in SolidWorks.

Data Availability Statement: The data presented in this study are available on request from the second author. The data are not publicly available due to restrictions apply to the availability of these data.

Acknowledgments: The authors would like to acknowledge their colleagues in the Division of Solid Mechanics (Lund University) for their valuable comments regarding mandibular fracture issues and also the management team at IKEA of Sweden for their fruitful discussions on the Six Sigma concepts during the second author’s stay from October to December 2020 at IKEA (Älmhult, Sweden).

Conflicts of Interest: All authors declare that the research was conducted in the absence of any commercial or financial relationships that could be construed as a potential conflict of interest.

References

1. Collette, Y.; Siarry, P. Multiobjective optimization: Principles and case studies. Principles and Case Studies. In *Book Series: Decision Engineering*; Springer: Berlin/Heidelberg, Germany, 2004.
2. Barker, R.M.; Puckett, J.A. Principles of Probabilistic Design. In *Design of Highway Bridges*; Wiley: Hoboken, NJ, USA, 2013.
3. Garg, H.; Ram, M. *Engineering Reliability and Risk Assessment*; Elsevier: Amsterdam, The Netherlands, 2023.
4. Blackburn, T.D. *Six Sigma: A Case Study Approach Using Minitab*; Springer Nature: Berlin/Heidelberg, Germany, 2022.
5. McClusky, R. The rise, fall and revival of Six Sigma quality. *Meas. Bus. Excell.* **2000**, *4*, 6.
6. Shafer, S.M.; Moeller, S.B. The effects of Six Sigma on corporate performance: An empirical investigation. *J. Oper. Manag.* **2012**, *30*, 521–532. [[CrossRef](#)]
7. Sanhita, N.H.; Vivek, D. A Review of Successful Implementation of Six Sigma in Different Industries-Methodology, Tools & Techniques Used, Benefits and Critical Success Factors. *Int. J. Adv. Eng. Res.* **2016**, *3*, 187–193.
8. Yadav, N.; Mathiyazhagan, K.; Kumar, K. Application of Six Sigma to minimize the defects in glass manufacturing industry: A case study. *J. Adv. Manag. Res.* **2019**, *16*, 594–624. [[CrossRef](#)]
9. Niñerola, A.; Sánchez-Rebull, M.V.; Hernández-Lara, A.B. Quality improvement in healthcare: Six Sigma systematic review. *Health Policy* **2020**, *124*, 438–445. [[CrossRef](#)]
10. Kapoor, A.; Bhaskar, R.; Vo, A. Pioneering the health care quality improvement in India using Six Sigma: A case study of a northern India hospital. *J. Cases Inf. Technol. (JCIT)* **2012**, *14*, 41–55. [[CrossRef](#)]
11. Silich, S.J.; Wetz, R.V.; Riebling, N.; Coleman, C.; Khoueiry, G.; Abi Rafeh, N.; Bagon, E.; Szerszen, A. Using six sigma methodology to reduce patient transfer times from floor to critical-care beds. *J. Healthc. Qual.* **2012**, *34*, 44. [[CrossRef](#)] [[PubMed](#)]
12. Udayai, K.; Kumar, P. Implementing Six Sigma to improve hospital discharge process. *Int. J. Pharm. Sci. Res.* **2012**, *3*, 4528.
13. Liberatore, J.M. Six Sigma in healthcare delivery. *Int. J. Health Care Qual. Assur.* **2013**, *26*, 601–626. [[CrossRef](#)]

14. Gijo, E.V.; Antony, J.; Hernandez, J.; Scaria, J. Reducing patient waiting time in a pathology department using the Six Sigma methodology. *Leadersh. Health Serv.* **2013**, *26*, 253–267. [[CrossRef](#)]
15. DelliFraine, J.L.; Wang, Z.; McCaughey, D.; Langabeer, J.R.; Erwin, C.O. The use of six sigma in health care management: Are we using it to its full potential? *Qual. Manag. Healthc.* **2014**, *23*, 240–253. [[CrossRef](#)] [[PubMed](#)]
16. Antony, J.; Palsuk, P.; Gupta, S.; Mishra, D.; Barach, P. Six Sigma in healthcare: A systematic review of the literature. *Int. J. Qual. Reliab. Manag.* **2018**, *35*, 1075–1092. [[CrossRef](#)]
17. Improta, G.; Ricciardi, C.; Borrelli, A.; D'alessandro, A.; Verdoliva, C.; Cesarelli, M. The application of six sigma to reduce the pre-operative length of hospital stay at the hospital Antonio Cardarelli. *Int. J. Lean Six Sigma* **2020**, *11*, 555–576. [[CrossRef](#)]
18. Rathi, R.; Vakharia, A.; Shadab, M. Lean six sigma in the healthcare sector: A systematic literature review. *Mater. Today Proc.* **2022**, *50*, 773–781. [[CrossRef](#)] [[PubMed](#)]
19. Kharmanda, M.G.; Kharma, M.Y.; Ristinmaa, M.; Wallin, M. Structural optimization of mini-plates in fixation of human mandible fractures. In Proceedings of the Nordic Seminar on Computational Mechanics, Stockholm, Sweden, 22–24 October 2014.
20. Kharmanda, G.; Kharma, M.Y. Evaluating the effect of minimizing screws on stabilization of symphysis mandibular fracture by 3D finite element analysis. *J. Maxillofac. Oral Surg.* **2017**, *16*, 205–211. [[CrossRef](#)] [[PubMed](#)]
21. Kharmanda, G.; Shokry, A.; Kharma, M.Y. Integration of reliability analysis into mini-plate fixation strategy used in human mandible fractures: Convalescence and healing periods. *Acta Bioeng. Biomech.* **2017**, *19*, 13–23.
22. Korkmaz, H.H. Evaluation of different miniplates in fixation of fractured human mandible with the finite element method. *Oral Surg. Oral Med. Oral Pathol. Oral Radiol. Endodontol.* **2007**, *103*, 1–137. [[CrossRef](#)]
23. Kharmanda, G. Reliability analysis for cementless hip prosthesis using a new optimized formulation of yield stress against elasticity modulus relationship. *Mater. Des.* **2015**, *65*, 496–504. [[CrossRef](#)]
24. Doblaré, M.; Garcia, J.M.; Gómez, M.J. Modelling bone tissue fracture and healing: A review. *Eng. Fract. Mech.* **2004**, *71*, 1809–1840. [[CrossRef](#)]
25. Mesnard, M.; Ramos, A.; Ballu, A.; Morlier, J.; Cid, M.; Simoes, J.A. Biomechanical analysis comparing natural and alloplastic temporomandibular joint replacement using a finite element model. *J. Oral Maxillofac. Surg.* **2011**, *69*, 1008–1017. [[CrossRef](#)]
26. Ramos, A.; Marques, H.; Mesnard, M. The effect of mechanical properties of bone in the mandible, a numerical case study. *Adv. Biomech. Appl.* **2014**, *1*, 67–76.
27. Evans, J.R.; Lindsay, W.M. An introduction to Six Sigma and process improvement. In *Cengage Learning*; Cengage Learning, Inc.: Florence, NC, USA, 2014.
28. Habbab, A.; Dayyeh. Statistical distributions and tests, and their applications in reliability evaluation. In *Chapter 4, Report of Reliability & Maintenance, Industrial Engineering Project*; University of Aleppo: Aleppo, Syria, 2005; pp. 37–62.
29. Gross, S.T.; Abel, E.W. A finite element analysis of hollow stemmed hip prostheses as a means of reducing stress shielding of the femur. *J. Biomech.* **2001**, *34*, 995–1003. [[PubMed](#)]
30. Tsarouhas, P.H. Reliability, availability, and maintainability analysis of an industrial plant based on Six Sigma approach: A case study in plastic industry. In *The Handbook of Reliability, Maintenance, and System Safety through Mathematical Modeling*; Elsevier: Amsterdam, The Netherlands, 2021; pp. 1–17.
31. Fonseca, R.J. Oral and Maxillofacial Surgery. *Saunders* **2017**, *2*, 146–172.
32. Draper, E.R.C. Basic biomechanics. In *Sciences Basic to Orthopaedics*; Spf, H., Id, M.C., Eds.; WB Saunders Company Limited: London, UK, 1998; Chapter 14; pp. 201–212, 447.
33. Champy, M.; Lodde, J.P.; Schmitt, R.; Jaeger, J.H.; Muster, D. Mandibular osteosynthesis by miniature screwed plates via a buccal approach. *J. Maxillofac. Surg.* **1978**, *6*, 14–21. [[CrossRef](#)]
34. Graillon, N.; Foletti, J.M.; Godio-Raboutet, Y.; Guyot, L.; Varazzani, A.; Thollon, L. Mandibular Titanium Miniplates Change the Biomechanical Behaviour of the Mandible in the Case of Facial Trauma: A Three-Dimensional Finite Element Analysis. *Bioengineering* **2023**, *10*, 994.
35. Kharmanda, G.; El-Hami. *Chapter 6—Integration of Reliability and Structural Optimization into Prosthesis Design, Biomechanics: Optimization, Uncertainties and Reliability (Reliability of Multiphysical Systems Set, 5, Band 5) Hardcover—Illustrated*; ISTE & Wiley: London, UK, 2017.
36. Atilgan, S.; Erol, B.; Yaman, F.; Yilmaz, N.; Ucan, M.C. Mandibular fractures: A comparative analysis between young and adult patients in the southeast region of Turkey. *J. Appl. Oral Sci.* **2010**, *18*, 17–22.
37. Frimpong, P.; Nguyen, T.T.H.; Sodnom-Ish, B.; Nimatu, E.S.; Dampare, N.Y.A.; Rockson, R.; Awuah, S.B.; Amponsah, E.K.; Newton, C.; Kim, S.M. Incidence and management of mandibular fractures in a low-resource health facility in Ghana. *J. Korean Assoc. Oral Maxillofac. Surg.* **2021**, *47*, 432–437.

Disclaimer/Publisher's Note: The statements, opinions and data contained in all publications are solely those of the individual author(s) and contributor(s) and not of MDPI and/or the editor(s). MDPI and/or the editor(s) disclaim responsibility for any injury to people or property resulting from any ideas, methods, instructions or products referred to in the content.